Numerical Investigation of the Laser Pulse Self-Guiding Through Air in Multiphoton Ionization Regime

Shadi Davoudi and Somayeh Mehrabian*

[a]Faculty of Physics, Shahrood University of Technology, Shahrood, Iran

Corresponding author email: s_mehrabian@shahroodut.ac.ir

Regular paper: Received: Aug. 06, 2022, Revised: Nov. 19, 2022, Accepted: Nov. 29, 2022,
Available Online: Dec. 01, 2022, DOI: 10.52547/ijop.16.1.107

ABSTRACT— In this study, the self-guiding of an ultrashort laser pulse through air is investigated. Therefore, the terms of self-focusing, plasma defocusing and the pulse energy depletion due to the ionization, are considered in the wave equation. Then the laser pulse spot size equation is obtained using the source-dependent expansion method. Our results show that the laser pulse self-guiding occurs for the first twenty Rayleigh lengths. However, the laser pulse undergoes diffraction as it propagates further along the *z* axis. Moreover, it is seen that the back of the laser pulse is diffracted the most owing to the fact that the plasma is formed as the laser pulse propagates through air. It is also shown that the spot size variations affect the temporal and spatial profiles of the laser intensity, the laser pulse power and the ionization process.

KEYWORDS: Laser spot size, Multiphoton ionization, Plasma defocusing, Self-focusing, Self-guiding.

I. INTRODUCTION

In the interaction of high-intensity laser pulses with a gas, there is a possibility of non-linear phenomena due to the plasma generation [1]-[2]. So that the combined effects of diffraction, self-focusing, ionization and the resultant plasma formation play an important role in the laser pulse propagation [3]-[9]. Laser beam propagation over long distances has many applications such as X-ray production, remote sensing, Raman amplification in plasmas, high harmonic generation, formation of long filaments in the atmosphere, THz radiation and etc. [3]-[8]. However, due to the effects of diffraction and plasma formation, which cause the divergence of the laser pulse, it is not possible for the pulse to propagate more than a few Rayleigh lengths (the length in which the beam propagates without noticeable divergence) [3]-[8]. On the other hand, the effects of diffraction and the plasma defocusing can be balanced by the laser pulse self-focusing in which the medium acts as a converging lens due to its nonlinear properties.

In the interaction of the ultrashort laser pulses with gas, the generated plasma increases the electron density which causes the refractive index reduction resulting in the laser pulse defocusing. On the other hand, increment of the relativistic mass of the electron and the decrement of the axial electron density caused by the ponderomotive force increase the refractive index which results in the focusing of the laser pulse. Therefore, if the effects of the self-focusing, diffraction and the plasma defocusing cancel out, the laser pulse propagates for long distances without convergence or divergence. This phenomenon is called the laser pulse self-guiding [3]-[9].

Self-channeling of a femtosecond laser pulse into filaments and its resultant propagation through distances greater than 20 m was first observed by Braun, *et al.* in 1995 [10]. Their work was followed by several experimental studies in which the self-guiding of the laser pulse or the generated plasma channels (as a result of the laser self-guiding) were investigated under different conditions [6]-[9], [11]-[12]. The application of these phenomena

[Downloaded from ijop.ir on 2026-11-23]

for the triggering and guiding of the electric discharge or the weather control were also studied [13]-[16].

On the theoretical side, some studies investigated the propagation of ultrashort laser pulses under the effects of different linear and nonlinear processes in which the self-guiding of a laser pulse was also investigated in a background gas (N_2 for instance) [2], [17]. The other works studied the self-focusing and guiding of a laser pulse in an ionizing gas or investigated the formed plasma channels in the tunneling ionization regime [3]-[4], [18]. However, as some of the main applications of the laser pulse self-guiding (including lightening protection and control, atmospheric remote sensing, weather control and induced lightening involving the rain or snow initiation) are based on the laser pulse self-guiding and its filamentation in air [13]-[16], and also due to the nonlinear nature of the process, there is a need to investigate the process in air instead of a background gas.

Therefore, in this study, the self-guiding of an ultrashort laser pulse in air ($0.8N_2$+$0.2O_2$) is investigated. For this purpose, the terms of plasma defocusing, self-focusing, and the pulse energy depletion due to the ionization are kept in the general equation of the laser pulse propagation. Then the equation of the laser spot size is obtained using the source-dependent expansion (SDE) method. This equation is numerically solved and the temporal and spatial distributions of the normalized laser spot size, power and intensity are given.

It is noteworthy that in the short and intense laser-matter interactions, the ionization regime is determined based on the value of the Keldysh adiabaticity parameter which is defined as $\gamma = \sqrt{U_{ion} / 2\varepsilon_q}$ in which ε_q is the quiver energy of the electrons in the laser field. If γ<1, the ionization occurs in the tunneling ionization regime while the multi photon ionization would be the ionization mechanism for γ>1. As in our work, the Keldysh adiabaticity parameter is greater than one, hence the ionization occurs in the multiphoton ionization regime [1]-[4].

Our results are applicable for the prediction of the optimum conditions for the laser pulse self-guiding to occur.

II. MATHEMATICAL MODEL

A. *The Governing Equations*

To investigate the self-guiding mechanism of a laser pulse, the 3-D propagation equation of a laser pulse in a nonlinear medium, with the terms of laser self-focusing (Kerr effect), the plasma defocusing and the pulse energy depletion due to the ionization, is used. With the transformation of variables from (z,t) to (z,τ), where $\tau = t - z / v_g$ (v_g is the group velocity of the laser pulse), the propagation equation becomes as follows [2], [17]:

$$\left(\nabla_{\perp}^2 + 2ik_0 \frac{\partial}{\partial z}\right) \mathrm{A}(r,z,\tau) = \left[-\frac{\omega_0^2 n_0{}^2 \eta_2}{4\pi c} |\mathrm{A}|^2 + \frac{\omega_p^2}{c^2} - \right.$$

$$\left. -8\pi i k_0 \frac{U_{ion}}{c|\mathrm{A}|^2} \frac{\partial n_e}{\partial \tau} \right] \mathrm{A}(r,z,\tau) \qquad (1)$$

where $\mathrm{A}(r,z,\tau)$, U_{ion}, n_0, n_e, c, ω_p, k_0 and ω_0 are the complex amplitude of the laser electric field, the ionization energy of the gas, the linear refractive index of the medium, the electron density, the light speed, the plasma frequency, the wavenumber and the frequency of the laser pulse, respectively. η_2 is also related to the nonlinear part of the refractive index. It is noteworthy that the first, second and third terms on the right-hand side of Eq. 1 refer to the laser pulse self-focusing, the plasma defocusing and the pulse energy depletion due to the ionization, respectively.

The complex amplitude of the laser electric field is defined as Eq. 2:

$$\mathrm{A}(r,z,\tau) = \mathrm{B}(z,\tau) \exp\left\{ i\theta(z,\tau) - \left[1 + i\alpha(z,\tau)\right] r^2 / r_s^2(z,\tau) \right\} \qquad (2)$$

where $\mathrm{B}(z,\tau)$, $\theta(z,\tau)$, and r_s are the electric field amplitude, phase and the laser spot size and α is related to the laser beam curvature. Using the SDE method and by defining

[Downloaded from ijop.ir on 2026-11-23]

$$\mathrm{M}(r,z,\tau)=-\frac{\omega_0^2 n_0{}^2\eta_2}{4\pi c}|\mathrm{A}|^2+\frac{\omega_p^2}{c^2}-8\pi i k_0\frac{U_{ion}}{c|\mathrm{A}|^2}\frac{\partial n_e}{\partial\tau} \tag{3}$$

$$\chi=-2r^2/r_s^2 \tag{4}$$

$$F(z,\tau)=\frac{1}{2k_0}\int_0^\infty \mathrm{M}(r,z,\tau)e^{-\chi}d\chi \tag{5}$$

$$G(z,\tau)=\frac{1}{2k_0}\int_0^\infty \mathrm{M}(r,z,\tau)(1-\chi)e^{-\chi}d\chi \tag{6}$$

where the following equations for B, θ, r_s and α are obtained [2].

$$\frac{1}{\mathrm{B}r_s}\frac{\partial(\mathrm{B}r_s)}{\partial z}=F_i \tag{7}$$

$$\frac{\partial\theta}{\partial z}+\frac{(1+\alpha^2)}{k_0 r_s^2}+\frac{\alpha}{r_s}\frac{\partial r_s}{\partial z}=-F_r \tag{8}$$

$$\frac{1}{r_s}\frac{\partial r_s}{\partial z}+\frac{2\alpha}{k_0 r_s^2}=-G_i \tag{9}$$

$$\frac{1}{2}\frac{\partial\alpha}{\partial z}+\frac{(1+\alpha^2)}{k_0 r_s^2}=-G_r-\alpha G_i, \tag{10}$$

where *i* and *r* indices refer to the real and imaginary parts of *F* and *G*.

It is noteworthy that the electron density obeys the following equation [2], [17]:

$$\frac{\partial n_e}{\partial t}=W\,n_n \tag{11}$$

where W and n_n are the ionization rate and the background neutral density, respectively.

Using the multiphoton ionization rate for air,

$$W=W_{mp}=\frac{2\pi\omega_0}{(l-1)!}\left(\frac{I(r,z,\tau)}{I_{mp}}\right)^l \tag{12}$$

$$W_{mp,air}=0.8W_{mp,N_2}+0.2W_{mp,O_2} \tag{13}$$

and using $n_e(r,z,\tau)=n_{e0}(z,\tau)\exp(-2lr^2/r_s{}^2)$, on the axis electron density equation becomes:

$$\frac{\partial n_{e0}(z,\tau)}{\partial\tau}=\left\{\frac{0.4\pi\omega}{(\ell_{o_2}-1)!}\left(\frac{\mathrm{I}(z,\tau)}{\mathrm{I}_{mp}}\right)^{\ell_{O_2}}+\frac{1.6\pi\omega}{(\ell_{N_2}-1)!}\left(\frac{\mathrm{I}(z,\tau)}{\mathrm{I}_{mp}}\right)^{\ell_{N_2}}\right\}n_n \tag{14}$$

where, *l* is the number of photons needed for the multiphoton ionization to happen and $I_{mp}=\hbar\omega_0{}^2/\sigma_{mp}$.

Using the laser power equation $\left(p(z,\tau)=cr_s^2\mathrm{B}^2/16\right)$ along with Eqs. 3-14, the following equations are derived for the laser pulse power [2], [17], and the laser spot size.

$$\frac{\partial p(z,\tau)}{\partial z}=-\frac{\pi n_n}{2}r_s^2(z,\tau)\left\{\frac{U_{ion(o_2)}}{\ell_{o_2}}\frac{0.4\pi\omega}{(\ell_{o_2}-1)!}\left(\frac{\mathrm{I}(z,\tau)}{\mathrm{I}_{mp}}\right)^{\ell_{o_2}}+\frac{U_{ion(N_2)}}{\ell_{N_2}}\frac{1.6\pi\omega}{(\ell_{N_2}-1)!}\left(\frac{\mathrm{I}(z,\tau)}{\mathrm{I}_{mp}}\right)^{\ell_{N_2}}\right\} \tag{15}$$

$$\frac{\partial^2 r_s(z,\tau)}{\partial z^2}=\frac{4}{k_0^2 r_s^3(z,\tau)}\left\{1-\frac{p(z,\tau)}{p_{NL}}+2\pi r_e r_s^2(z,\tau)\left[\frac{\ell_{o_2}}{(\ell_{o_2}+1)}n_{e0(o_2)}(z,\tau)+\frac{\ell_{N_2}}{(\ell_{N_2}+1)}n_{e0(N_2)}(z,\tau)\right]\right\}-\frac{1}{r_s^3(z,\tau)}\left\{\left(\frac{\ell_{o_2}-1}{2\ell_{o_2}}+\frac{\ell_{N_2}-1}{2\ell_{N_2}}\right)\right.$$

[Downloaded from ijop.ir on 2026-11-23]

$$\left[\left(\frac{\ell_{o_2}-1}{2\ell_{o_2}}\right)^2+\left(\frac{\ell_{N_2}-1}{2\ell_{N_2}}\right)^2\right]\left[\frac{r_s^2(z,\tau)}{p(z,\tau)}\frac{\partial p(z,\tau)}{\partial z}\right]^2\Bigg\} \quad (16)$$

where $P_{NL}=\lambda^2/(2\pi\eta_2)$ is the nonlinear focusing power, $r_e=q^2/mc^2$ is the classical electron radius and $\mathrm{I}(z,\tau)=2p(z,\tau)\big/\pi r_s^2(z,\tau)$.

B. *The Numerical Method*

To investigate the variations of the laser pulse spot size, Eqs. 14-16 are numerically solved using the finite difference method. The used initial and boundary conditions are as follows;

$$P(z=0,\tau)=P_{NL}\left\{1+2\pi r_e r_s^2(0,\tau)\frac{-b\pm\sqrt{b^2-4ac}}{2a}\times\left[\frac{\ell_{o_2}}{(\ell_{o_2}+1)}n_{e0(o_2)}(0,\tau)+\frac{\ell_{N_2}}{(\ell_{N_2}+1)}n_{e0(N_2)}(0,\tau)\right]\right\} \quad (17)$$

$$I(z=0,\tau)=2P(0,\tau)/\pi r_s^2(0,\tau) \quad (18)$$

$$I(z,\tau=0)=I_0,\quad n_e(0,0)=0, \quad (19)$$

$$r_s\big|_{z=0}=r_0,\ \text{and}\ \partial r_s/\partial z\big|_{z=0}=0 \quad (20)$$

while the model parameters are listed in the following table.

III. RESULTS AND DISCUSSION

The spatial distribution of the normalized laser spot size at τ=0, 15, and 120 fs with and without inclusion of the pulse energy depletion (the third term on the right-hand side of Eq. 1 is depicted in Fig. 1. It is noteworthy that the laser spot size is normalized to r_0 and the distances along the z axis are also normalized to the Rayleigh length (z_r).

As it is clear, the pulse undergoes diffraction as it propagates along the z axis. To be more precise, the laser pulse spot size remains almost constant (normalized spot size is approximately equal to 1) up to z=20z_r and then the laser pulse starts to diffract. This implies that the laser self-guiding occurs up to z=20z_r after which the diffracting factors dominate the optical Kerr effect and its resultant self-focusing influence. This is due to the fact that the natural diffraction increases with the laser pulse propagation along the z axis. Moreover, the plasma density increases as the laser pulse passes through. Therefore, the defocusing effect of the plasma increases leading to the spot size increment with z.

Table 1. The model parameters

Parameter	Value
λ	0.775 μm
r_0	50 μm
η_2	5.6×10^{-19} cm^2/W
I_0	4.3×10^{13} W/cm^2
σ_{mp}	6.4×10^{-18} cm^2
U_{ion} (N_2)	15.6 eV
U_{ion} (O_2)	12.1 eV
Pulse Duration	120 fs
dt	120×10^{-18} s
dz	0.01 cm

Moreover, as τ=0 and 120 fs, indicates the front and back of the laser pulse, it is seen that the diffraction occurs with a faster rate for the back of the laser pulse. This is due to the fact that the air starts to ionize as the laser pulse passes through; therefore, the back of the pulse is affected more by the formed plasma and its defocusing effect and as a result, it is diffracted more in comparison with the laser pulse front. In addition, as the laser pulse starts to diffract from its front and back; thus, the time of τ=15 fs which is within the body of the laser pulse, has the slowest diffraction rate.

The temporal distribution of the normalized spot size at z=10z_r, 25z_r and 40z_r with and without inclusion of the pulse energy depletion is shown in Fig. 2. As it is clear, the laser pulse spot size is almost constant with τ for $z=10z_r$ which is due to the fact that at the early stages of the laser pulse propagation, the plasma density is not high enough to defocus the laser

[Downloaded from ijop.ir on 2026-11-23]

pulse effectively and as a result, the laser pulse self-guiding occurs approximately up to $z=20z_r$ (Fig. 1). Therefore, it is expected that the spot size variations become more pronounced for $z>20z_r$. This fact is clear in parts (b) and (c) of the figure. At $z = 25z_r$, the normalized spot size varies between 0.92 and 1.31 while the variation becomes more noticeable for $z=40z_r$ in which the spot size varies between 0.95 and 2.94. This confirms the increment of the pulse diffraction with distance.

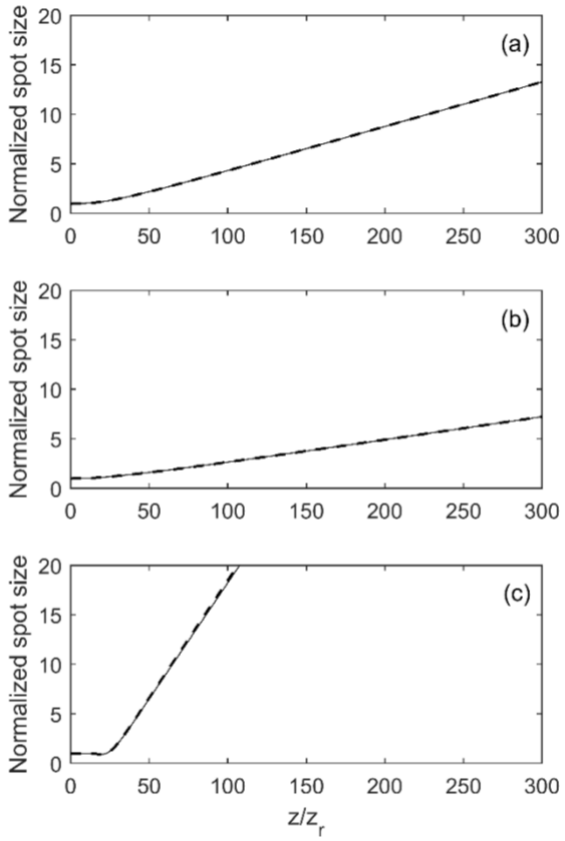

Fig. 1. The spatial distribution of the normalized laser spot size at (a) τ=0, (b) τ=15 fs, and (c) τ=120 fs with inclusion (solid line) and without inclusion (dashed line) of the pulse energy depletion.

Moreover, due to the fact that the pulse starts to diffract from its front and back, it is expected that the minimum of the normalized spot size occurs within the body of the laser pulse in comparison with its front (τ=0 fs) and back (τ=120 fs). The existence of these minimums is clearly noticeable in parts (b) and (c) of the figure which is also in accordance with the results presented in Fig. 1.

Paying attention to Figs. 1 and 2, it is clear that the pulse energy depletion does not have an effective role in the laser pulse self-guiding. As it is seen, the obtained curves with and without inclusion of the pulse energy depletion (solid and dashed lines in all panels of both figures) are almost the same.

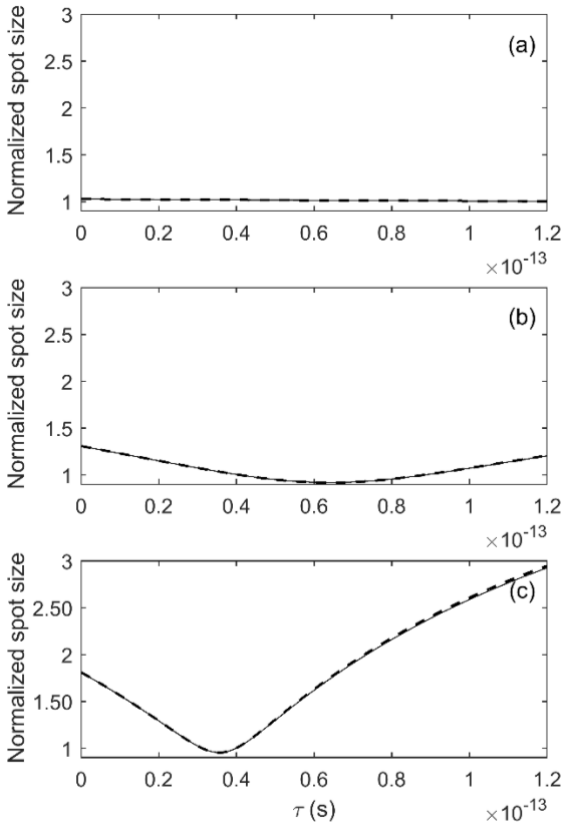

Fig. 2. The temporal distribution of the normalized spot size at (a) $z=10z_r$, (b) $z=25z_r$, and (c) $z=40z_r$ with inclusion (dashed line) and without inclusion (solid line) of the pulse energy depletion.

In order to compare the obtained result with the normalized laser pulse spot size in an ionizing gas, the laser pulse self-guiding was also investigated in the Nitrogen (N_2) and Oxygen (O_2) gases, respectively. The spatial and temporal distributions of the obtained results are presented in Figs. 3 and 4.

Figure 3 shows the spatial distributions of the normalized laser spot size in Oxygen and Nitrogen gases at τ=0, 15, and 120 fs. As it is observed, the laser pulse undergoes diffraction as it propagates along the z axis in both of the Oxygen and Nitrogen gases which is expected. It is due to the increment of the plasma density

[Downloaded from ijop.ir on 2026-11-23]

with the interaction length which is the same as what was observed in air.

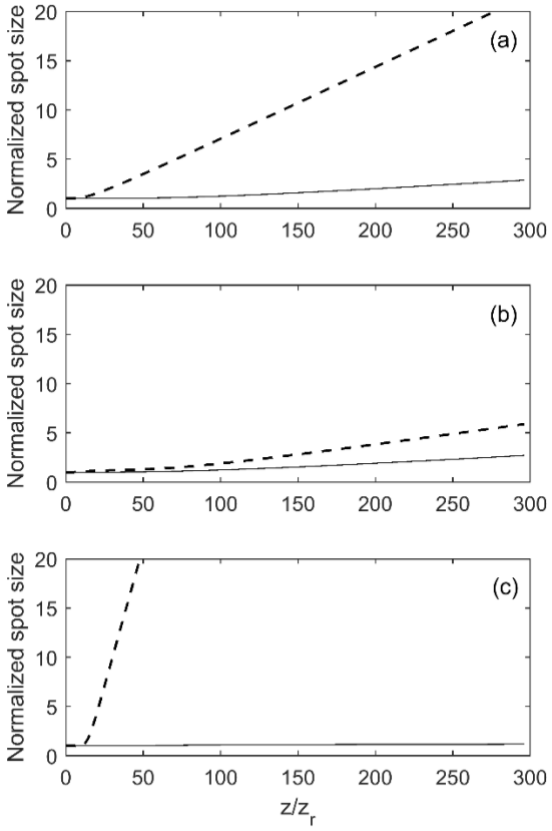

Fig. 3. The spatial distribution of the normalized laser spot size at τ=0 (a), τ=15 (b) and τ=120 fs (c) in Oxygen (dashed line) and Nitrogen (solid line) gases.

Paying attention to the Oxygen curves, it is seen that the normalized spot size increases with a faster rate at the back of the pulse while it has its lowest values within the body of pulse. This is the trend which was also observed for air. It implies that the gas starts to ionize as the laser pulse passes through and as a result, the back of the laser pulse is affected more by the plasma defocusing effect. Moreover, as the laser pulse starts to diffract from its front and back; thus, the time of τ=15 fs which is within the body of the laser pulse, has the lowest diffraction.

In addition, it is seen that the laser pulse has the lowest divergence while propagating in the Nitrogen gas whereas the highest diffraction occurs for the Oxygen. The reason is due to the fact that the Nitrogen gas has the highest ionization energy (15.6 eV) among these three mediums, while the Oxygen holds the lowest value (12.1 eV). Thus, the Oxygen gas undergoes ionization simply, in comparison with the air and the Nitrogen gas and as a result, the plasma forms more easily in the case of Oxygen which in turn has a pronounced defocusing effect. Comparing figures 1 and 3, it is seen that the laser pulse divergence in air, is larger than its divergence in Nitrogen and also smaller than the Oxygen gas.

The temporal distribution of the normalized laser spot size at z=10z_r, 25z_r, and 40z_r in the Oxygen and Nitrogen gases is presented in Fig. 4. As the laser pulse spot size is almost constant up to z=10z_r for both of the Oxygen and Nitrogen gases (Fig. 3), it is expected that the laser spot size dose not vary with τ at z=10z_r which is clearly seen in Fig. 3(a). However, the spot size has a slight variation for the oxygen which is due to its lower ionization energy.

Moreover, as the laser spot size increases with the interaction length, it is expected that the spot size starts to vary with τ as z increases. This is the trend which is obvious in parts (b) and (c) of the figure. Therefore, it is expected that the spot size variations become more pronounced for z=40z_r.

In addition, regarding the fact that the laser pulse diffraction is minimized within the body of the laser pulse while it is maximized at the back of the laser pulse, it is seen that the maximum of the normalized laser spot size occurs at τ=120 fs. The maximum values, in Oxygen gas, at z=25z_r and z=40z_r, are 3.64 and 6.94 respectively; whereas the normalized spot size becomes minimized within the pulse with the values of 0.95 and 1.12 at z=25z_r and z=40z_r, respectively. It is noteworthy the spot size variations for the Nitrogen gas are relatively small in comparison with the Oxygen which is due to the its high ionization energy.

Figure 5 shows the spatial distribution of the normalized laser intensity (it is normalized to I_0) at τ=0, 15, and 120 fs. The laser intensity is defined as the power per unit area delivered by the laser pulse. Hence, the laser pulse spot size affects the laser intensity and as a result, it is expected that the laser intensity decreases as the laser spot size increases.

[Downloaded from ijop.ir on 2026-11-23]

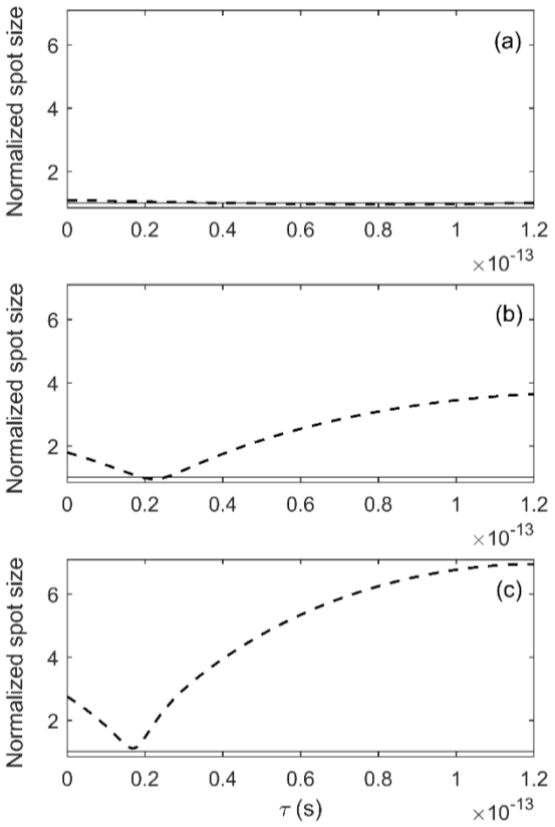

Fig. 4. The spatial distribution of the normalized laser spot size at (a) $z=10z_r$, (b) $z=25z_r$, and (c) $z=40z_r$ in Oxygen (dashed line) and Nitrogen (solid line) gases.

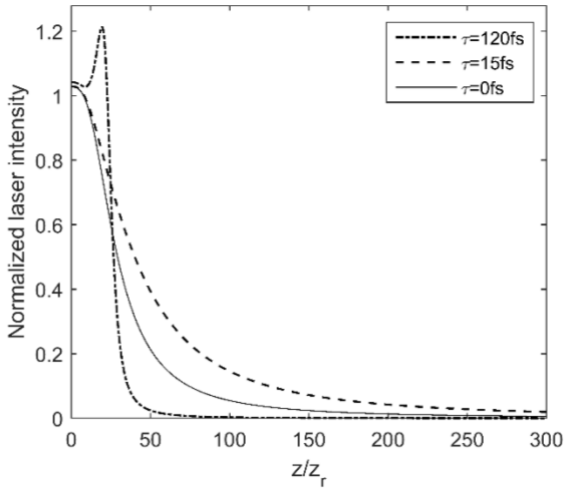

Fig. 5. The spatial distribution of the normalized laser intensity at $\tau=0$ (dashed line), $\tau=15$ (dotted line) and $\tau=120$ fs (solid line).

Therefore, as the laser spot size increases with the propagation distance, it is expected that the laser intensity decreases as the laser propagates along the z axis. The trend obvious in Fig. 5 for all the curves. Moreover, the most intensity decrement is observed for the back of the laser pulse ($\tau=120$ fs) which is diffracted the most while the slightest intensity decrement occurs for $\tau=15$ fs which is diffracted the least.

The temporal distribution of the normalized laser intensity at $z=10z_r$, $25z_r$, and $40z_r$ is shown in Fig. 6. As it is seen, the laser intensity has a slight variation with τ at $z=10z_r$; which is due to the fact that laser spot size does not vary with τ and is almost constant at this point. However, the intensity variations become more pronounced at $z=25z_r$ which is due to the more spot size variations at this point. It is also obvious that the laser intensity experiences a maximum at $\tau=64$ fs at which the laser spot size becomes minimum (Fig. 2). This trend, but with a wider intensity variation rang, is also observed at $z=40z_r$ with the maximum of the intensity located at $\tau=36$ fs in which the laser spot size has its minimum value (Fig. 2).

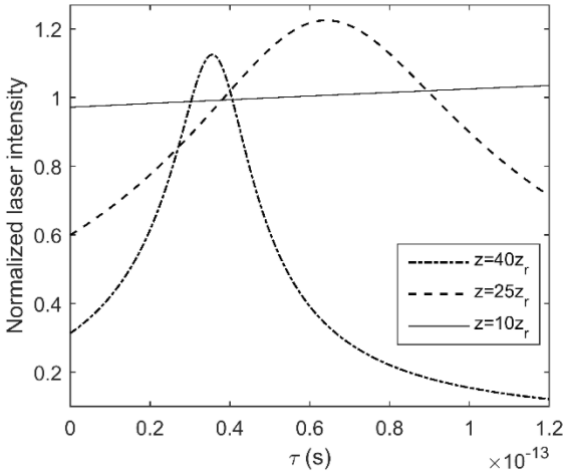

Fig. 6. The temporal distribution of the normalized laser intensity at $z=0$ (solid line), $z=10z_r$ (dashed line), $z=25z_r$ (dotted line) and $z=40z_r$ (dashed-dotted line).

Figure 7 shows the spatial distribution of the normalized laser power (it is normalized to P_{NL}) at $\tau=0$, 15, and 120 fs.

As it was stated in Fig. 1, the spot size remains almost unchanged up to $z=20z_r$ which within this range, the laser intensity does not vary significantly. Hence, the ionization takes place and the laser pulse power is depleted due to the ionization process. The decreasing trend of the laser power with z up to $z=20z_r$, is the indicator of the mentioned depletion. However, the laser

[Downloaded from ijop.ir on 2026-11-23]

pulse starts to diffract beyond $z=20z_r$ and as a result, the laser pulse intensity decreases significantly (Fig. 5). Therefore, the ionization process ceases and as a result, the laser pulse power does not deplete anymore and remains almost constant. This trend is obviously clear in the figure for τ=0, 15, and 120 fs.

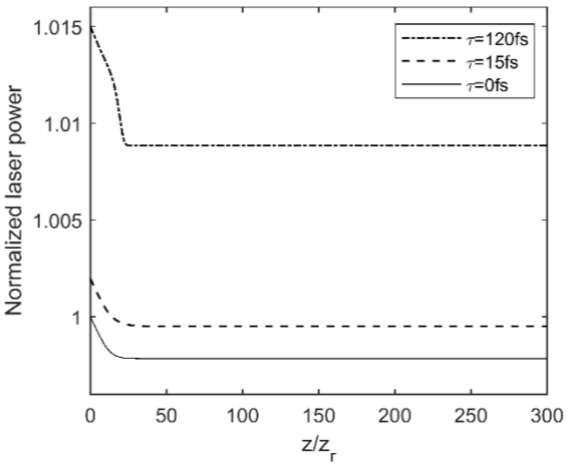

Fig. 7. The spatial distribution of the normalized laser power at τ=0 (solid line), τ=15 (dashed line) and τ=120 fs (dotted line).

The temporal distribution of the normalized laser power at $z=10z_r$, $25z_r$, and $40z_r$ is shown in Fig. 8.

As the laser intensity has slight variations with τ for $z=10z_r$ (Fig. 6), the air ionization occurs and as a result, the laser pulse power depletes and experiences a linear variation with τ. However, for $z>20z_r$, due to the nonlinear intensity variations (Fig. 6), the ionization process depletes the laser pulse power nonlinearly; which is clearly observable for $z=25z_r$ and $z=40z_r$ in the figure. Moreover, as the intensity variation range is wider for $z=40z_r$, the air ionization depletes the pulse power more significantly. This nonlinear depletion occurs within the body of the pulse which is due to the fact that the laser intensity and its consequent ionization are maximized within the pulse and hence, it is expected that that laser pulse power experiences a significant depletion within the pulse in comparison with its back and front.

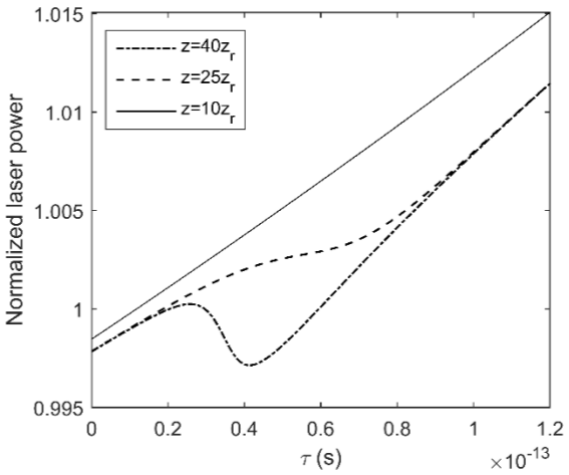

Fig. 8. The temporal distribution of the normalized laser power at z=0 (solid line), $z=10z_r$ (dashed line), $z=25z_r$ (dotted line) and $z=40z_r$ (dashed-dotted line).

IV. CONCLUSION

In this research, the self-guiding of an ultrashort laser pulse in air was studied in the multiphoton ionization regime. For this purpose, the terms of self-focusing, plasma defocusing and the pulse energy depletion due to the ionization were kept in the general form of the wave equation. Then the equation governing the laser pulse spot size was obtained using the source-dependent expansion (SDE) method and was solved numerically. Our results showed that the laser pulse self-guiding occurred for the first twenty Rayleigh lengths. However, the laser underwent diffraction as it propagated further along the z axis. Moreover, it was seen that the back of the laser pulse was diffracted the most which is due to the fact that the plasma was formed as the laser propagated through air. It was also shown that the spot size variations affected the temporal and spatial profiles of the laser intensity which in turn affected the air ionization influencing the laser pulse power. It was also observed that the ionization energy of the medium is a determining factor affecting the laser pulse diffraction. Our results are applied to the optimization of the laser pulse self-guiding in electric discharge and weather control, remote sensing, high harmonic and THz generation and etc.

[Downloaded from ijop.ir on 2026-11-23]

REFERENCES

[1] P. Sprangle, E. Esarey, and A. Ting. "Nonlinear interaction of intense laser pulses in plasmas," Phys. Rev. A, Vol. 41, pp. 4463-4469, 1990.

[2] P. Sprangle, J.R. Peñano, and B. Hafizi. "Propagation of intense short laser pulses in the atmosphere," Phys. Rev. E, Vol. 66, pp. 046418 (1-21), 2002.

[3] E. Esarey, P. Sprangle, J. Krall, and A. Ting. "Self-Focusing and Guiding of Short Laser Pulses in Ionizing Gases and Plasmas," IEEE J. Quantum Electron., Vol. 33, pp. 1879-1914, 1997.

[4] P. Sprangle, E. Esarey, and J. Krall. "Self-guiding and stability of intense optical beams in gases undergoing ionization," Phys. Rev. E, Vol. 54, pp. 4211-4232, 1996.

[5] P. Sprangle, B. Hafizi, J.R. Peñano, R.F. Hubbard, A. Ting, A. Zigler, and T.M. Antonsen, Jr. "Stable Laser-Pulse Propagation in Plasma Channels for GeV Electron Acceleration," Phys. Rev. Lett., Vol. 85, pp. 5110-5113, 2000.

[6] J. Zhu, Z. Ji, Y. Deng, J. Liu, R. Li, and Z. Xu, "Long lifetime plasma channel in air generated by multiple femtosecond laser pulses and an external electrical field," Opt. Express, Vol. 14, pp. 4915-4922, 2006.

[7] X. Lu, S.Y. Chen, J.L. Ma, L. Hou, G.Q. Liao, J.G. Wang, Y.J. Han, X.L. Liu, H. Teng, H.N. Han, Y.T Li, L.M Chen, Z.Y. Wei, and J. Zhang. "Quasi-steady-state air plasma channel produced by a femtosecond laser pulse sequence," Sci. Rep., Vol. 5, pp. 15515 (1-9), 2015.

[8] J. Liu, Z. Duan, Z. Zeng, X. Xie, Y. Deng, R. Li, Z. Xu, and S.L. Chin, "Time-resolved investigation of low-density plasma channels produced by a kilohertz femtosecond laser in air," Phys. Rev. E, Vol. 72, pp. 026412 (1-7), 2005.

[9] H. Yang, J. Zhang, Y. Li, J. Zhang, Y. Li, Z. Chen, H. Teng, Z. Wei, and Z. Sheng, "Characteristics of self-guided laser plasma channels generated by femtosecond laser pulses in air," Phys. Rev. E, Vol. 66, pp. 016406 (1-4), 2002.

[10] A. Braun, G. Korn, X. Liu, D. Du, J. Squier, and G. Mourou, "Self-channeling of high-peak-power femtosecond laser pulses in air," Opt. Lett., Vol. 20, pp. 73-75, 1995.

[11] A. Schmitt-Sody, H.G. Kurz, L. Bergé, S. Skupin, and P. Polynkin. "Picosecond laser filamentation in air," New J. Phys., Vol. 18, pp. 093005 (1-9), 2016.

[12] S. Tzortzakis, B. Prade, M. Franco, and A. Mysyrowicz, "Time-evolution of the plasma channel at the trail of a self-guided IR femtosecond laser pulse in air," Opt. Commun., Vol. 181, pp. 123-127, 2000.

[13] S. Tzortzakis, B. Prade, M. Franco, A. Mysyrowicz, S. Hüller, and P. Mora, "Femtosecond laser-guided electric discharge in air," Phys. Rev. E, Vol. 64, pp. 057401 (1-4), 2001.

[14] H.D. Ladouceur, A.P. Baronavski, D. Lohrmann, P.W. Grounds, and P.G. Girardi, "Electrical conductivity of a femtosecond laser generated plasma channel in air," Opt. Commun., Vol. 189, pp. 107-111, 2001.

[15] V.D. Zvorykin, A.A. Ionin, A.O. Levchenko, L.V. Seleznev, D.V. Sinitsyn, I.V. Smetanin, N.N. Ustinovskii and A.V. Shutov. "Extended plasma channels created by UV laser in air and their application to control electric discharges," Plasma Phys. Rep., Vol. 41, pp. 112-146, 2015.

[16] J.P. Wolf, "Short-pulse lasers for weather control," Rep. Prog. Phys., Vol. 81, pp. 026001 (1-34), 2018.

[17] J.R. Peñano, P. Sprangle, B. Hafizi, A. Ting, D.F. Gordon, and C.A. Kapetanakos, "Propagation of ultra-short, intense laser pulses in air," Phys. Plasmas, Vol. 11, pp. 2865- 2874, 2004.

[18] H. Yang, J. Zhang, W. Yu, Y.J. Li, and Z.Y. Wei. "Long plasma channels generated by femtosecond laser pulses," Phys. Rev. E, Vol 65, pp. 016406 (1-5), 2001.

[Downloaded from ijop.ir on 2026-11-23]



Shadi Davoudi was born in Esfarayen, Iran, on January 10, 1993. She received her B.Sc in nuclear physics in 2015 from Payam Noor University of Mashhad, Iran, and got her M.Sc degree in plasma physics in 2021 from Shahrood University of Technology, Shahrood, Iran.



Somayeh Mehrabian was born on February, 3, 1983 in Kerman, Iran. She got her B.Sc in applied physics from Shahid Bahonar University of Kerman, Iran in 2005. She also received her M.Sc and Ph.D. degrees in photonics from Shahid Beheshti University, Tehran, Iran in 2008 and 2013, respectively.

She is currently an assistant professor in Shahrood University of Technology. Her research interests are intense laser-plasma interactions, growth of nanostructures in plasmas, laser induced plasma breakdown and nonlinear optics.

[Downloaded from ijop.ir on 2026-11-23]